MOLECULAR AND CELLULAR BIOLOGY, Oct. 1997, p. 6049–6056 Vol. 17, No. 10
0270-7306/97/$04.00+0

HEC, a Novel Nuclear Protein Rich in Leucine Heptad Repeats Specifically Involved in Mitosis

YUMAY CHEN, DANIEL J. RILEY, PHANG-LANG CHEN, AND WEN-HWA LEE*

Department of Molecular Medicine, Institute of Biotechnology, University of Texas Health Science Center at San Antonio, San Antonio, Texas 78245

Received 18 April 1997/Returned for modification 28 May 1997/Accepted 2 July 1997

The protein encoded by the human gene *HEC* (highly expressed in cancer) contains 642 amino acids and a long series of leucine heptad repeats at its C-terminal region. HEC protein is expressed most abundantly in the S and M phases of rapidly dividing cells but not in terminal differentiated cells. It localizes to the nuclei of interphase cells, and a portion distributes to centromeres during M phase. Inactivation of HEC by microinjection of specific monoclonal antibodies into cells during interphase severely disturbs the subsequent mitoses. Disordered sister chromatid alignment and separation, as well as the formation of nonviable cells with multiple, fragmented micronuclei, are common features observed. These results suggest that the HEC protein may play an important role in chromosome segregation during M phase.

The ultimate goal of cell division is to ensure high-fidelity transmission of replicated DNA to daughter cells. The physical separation of pairs of sister chromatids into two daughter cells is orchestrated precisely during M phase, and many of the events involved are highly conserved in all eukaryotes (46). To ensure faithful progress through cell division, each step is coordinated by a group of structural and regulatory proteins that serve as checkpoints to monitor the timing and accuracy of previous steps (21). Mitotic B-type cyclins, cyclin-dependent kinases, other kinases, and components of the centromere/kinetochore have all received considerable attention (20, 22). Under normal circumstances, faulty cell cycle events will be sensed and cell cycle progression will stall until the problems can be resolved.

In addition to transcriptional control of gene expression and phosphorylation-dephosphorylation, progression of the cell cycle involves the targeted degradation of proteins regulating key transition points. Two key checkpoints in mitosis, sister chromatid separation and exit to G_1, are known to require the destruction of specific proteins such as anaphase inhibitory factors and mitotic cyclins (16, 24, 25). Degradation is accomplished primarily by a pathway that involves ubiquitination (reviewed in reference 10), a series of enzymatic modifications that mark proteins for destruction by a multiple-subunit protease called the proteasome.

Rapid progress has recently been made by using fungi, *Drosophila melanogaster*, and *Xenopus laevis* to dissect the molecular and cellular processes occurring during mitosis. Yeasts have been exploited in particular because of the relative ease with which their genes can be manipulated to select mutants defective in mitosis. Several genes that lead to M phase arrest have been isolated. Some encode proteins involved in the protein degradation process, e.g., CIM3 (Sug1) and CIM5, both subunits of the 26S proteasome in budding yeast (15, 40). Some, such as nuc2 (23) and cut9 (34) of fission yeast, are classified by sequences encoding tetratricopeptide repeat domains (17). Nuc2/CDC27Hs has recently been shown to associate with the centromere and mitotic spindle and to function in the ubiquitin-mediated protein degradation pathway (29, 41). Kinases such as NimA in *Aspergillus nidulans* (31) and phosphatases such as protein phosphatase type 1-alpha (11) also lead to mitotic arrest when inactivated. Other proteins, such as SMC1 and SMC2, are essential for chromosome segregation and condensation (38, 39); yet others, such as tubulin (44) and kinesin-like proteins (42), are required for spindle formation. Although the number of known proteins and genes required for chromatid separation is rapidly increasing, the precise mechanisms responsible for mitotic molecular events remain elusive. Recent evidence suggests that metaphase arrest induced by primary structural abnormalities in the kinetochore may also require interaction with proteins involved in spindle assembly and in monitoring of mitotic checkpoints (43, 45).

Investigations of the molecules involved in chromatid segregation and checkpoint control are important because aneuploidy, or alteration of chromosome number, is a common finding in neoplastic cells. Aneuploidy apparently results from improper chromosomal segregation in M phase (37). The strong association of aneuploidy with cancer suggests that altered regulation of the mitotic process also contributes substantially to oncogenesis and to tumor progression. In addition, defects of the ubiquitin-mediated proteolytic pathway may enhance genomic instability or cause loss of control of cell growth and proliferation by affecting the degradation of cyclins or cyclin-dependent kinase inhibitors (CKIs) (2). For example, the removal of mitotic checkpoints while preserving daughter cell viability could confer clonal growth advantages and eventually lead to cancer.

To aid in the exploration of the molecular events of mitosis and to help explain how the chromosomal abnormalities observed in malignant cells might originate, specific proteins crucial for mitotic progression must be identified, characterized, and linked to known pathways of mitotic protein regulation. To this end, we describe here the characterization of a human nuclear protein, HEC, which was isolated as clone 15 (C15) through its interaction with the retinoblastoma protein (Rb) in the yeast two-hybrid system (12). The HEC protein apparently plays an important role in chromosome segregation during M phase. It is expressed most abundantly in rapidly dividing cells, localizes to centromeres during mitosis, and, when inactivated,

* Corresponding author. Mailing address: Department of Molecular Medicine, Institute of Biotechnology, University of Texas Health Science Center at San Antonio, 15355 Lambda Dr., San Antonio, TX 78245. Phone: (210) 567-7353. Fax: (210) 567-7377.

leads to severe abnormalities in chromosome congression and segregation, resulting in nonviable cells.

MATERIALS AND METHODS

RNA blotting analysis. Total RNA extraction, poly(A) mRNA isolation, and RNA blotting analysis were performed by standard methods (35). The Gβ-like and E2F-1 mRNA probes have been described previously (35). Gβ-like mRNA is expressed constitutively and served as an internal loading control. Monkey kidney CV1 cells treated with drugs to enrich for distinct cell cycle stages were used for RNA extraction as described previously (35).

Isolation of full-length HEC cDNA. A 1.8-kb C15 cDNA fragment was originally cloned from a human B-cell cDNA library by its interaction with the C terminus of Rb in a yeast two-hybrid system (12). This fragment was then used as a probe to screen a λYES cDNA library. Several overlapping cDNA clones were obtained. The longest clone obtained, spanning ~2.3 kb, was ligated into pBKS to create pBKS-C15, from which the *HEC* cDNA was sequenced and from which the longest open reading frame was deduced.

Preparation of polyclonal and monoclonal anti-C15 antibodies. A glutathione *S*-transferase (GST)–C15 fusion protein containing amino acids 56 to 642 was created by ligating a unique *Xho*I-*Xho*I C15 cDNA fragment (nucleotides 264 to 2045) into a modified version of pGEX-3X (Pharmacia, Piscataway, N.J.) to create pGST-C15. The protein was expressed in *Escherichia coli* by induction with isopropyl-β-D-thiogalactopyranoside (IPTG; 0.1 mM) and purified with glutathione-Sepharose beads as described previously (5). Recovered protein, >95% pure, was then used as an antigen in mice. Serum from the immunized mice was preabsorbed on GST columns and used directly for immunoprecipitation, developing immunoblots, and immunostaining. Preimmune serum was obtained from the same mice and used at the same dilution (1:1,000). Monoclonal antibodies (MAbs) were prepared by standard procedures (19) and characterized as above.

In vivo metabolic labeling, in vitro transcription and translation. To label cellular proteins, T24 cells (5×10^6 for each lane) were grown to ~70% confluence and then incubated with [^{35}S]methionine (300 μCi) for 2 h. The cells were then lysed in Lysis 250 buffer for immunoprecipitation as described previously (8). For in vitro translation, the full-length *HEC* cDNA was inserted into pBKS and then transcribed and translated in the presence of [^{35}S]methionine with the TNT coupled reticulocyte lysate system (Promega, Madison, Wis.).

Cell cycle synchronization. Human T24 bladder carcinoma cells, grown in Dulbecco's modified Eagle's medium (DMEM)–10% fetal calf serum (FCS), were synchronized at G_1 by density arrest and then released at time zero by replating in DMEM–10% FCS at a density of 2×10^6 cells per 10-cm plate. At various time points thereafter (18 h for G_1/S, 22 h for S, 33 h for G_2), the cells were harvested. To obtain cells in M phase, nocodazole (0.4 μg/ml) was added to the culture medium for 8 h prior to harvest. Samples of cells were fixed in ethanol and analyzed by fluorescence-activated cell sorting to determine cell cycle phases as described previously (8).

Induction of terminal differentiation. Mouse 3T3/L1 fibroblasts were induced to differentiate as described previously (7). This process involved first growing cells to confluence and then, on day 0 of the differentiation induction program, exposing them to fresh DMEM–10% FBS–1 μM dexamethasone–10 μM forskolin–10 μg of insulin per ml for 48 h to initiate adipogenesis. The medium was then replaced with DMEM–10% FBS–10 μg of insulin per ml, and the cells were refed every other day until day 8. To confirm the appearance of the adipogenic phenotype, particularly the accumulation of neutral fat droplets in the cytoplasm, the cells were fixed at particular time points in 3% glutaraldehyde–100 mM sodium phosphate buffer (pH 7.4) and stained with Oil Red EGN. In the differentiation of large-cell lymphoma cells along the monocyte/macrophage lineage, U937 cells at an initial density of 5×10^5 per ml were incubated for 4 days in the presence of tetradecanoyl phorbol acetate (100 ng/ml). The macrophages were observed on day 4 as previously described (4).

Immunoprecipitation and Western blot analysis. Cell lysates in Lysis 250 buffer were subjected to three freeze-thaw cycles (freezing in liquid nitrogen and heating at 37°C) and clarified by centrifugation (10,000 × *g* for 2 min at room temperature). The supernatants were used for immunoprecipitation as described previously (8). Briefly, to each clarified supernatant was added 1 μl of mouse polyclonal anti-C15 antiserum. For competition experiments, antigens and antibodies were incubated together for 1 h before addition to the cell lysate. After a 1-h incubation, protein A-Sepharose beads were added for another 1 h. The beads were then collected, washed five times with lysis buffer containing 250 mM NaCl, and boiled in sodium dodecyl sulfate (SDS)-loading buffer for immunoblotting analysis as described previously (8).

Metaphase chromosome spreads. Cycling T24 cells were treated with nocodazole for 8 h. Mitotic cells were shaken off the culture plates and swollen in 75 mM KCl. Free chromosomes were then cytocentrifuged onto coverslips and incubated with a drop of the DNA-specific dye 4′,6-diamidino-2-phenylindole (DAPI) for 10 min. The same chromosomes were stained with anti-HEC and human autoimmune (CREST) antisera and then counterstained with fluorescein isothiocyanates or Texas Red-conjugated secondary antibodies. Digital photographs were obtained with a Zeiss microscope (magnification, ×400) and a Hamamatsu Photonics camera. The images were superimposed with Photoshop for Power MacIntosh software.

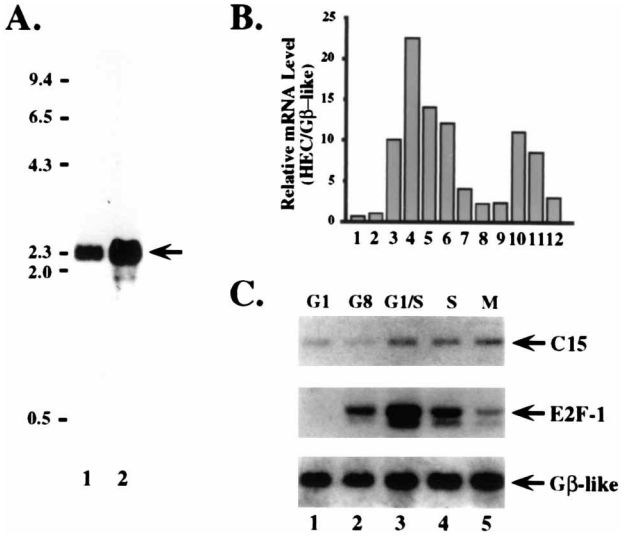

FIG. 1. *HEC* mRNA expression. (A) Northern blot analysis of poly(A)-selected RNA (2 μg each) from human brain (lane 1) and WERI-RB-27 retinoblastoma cells (lane 2), probed with a 1.8-kb fragment of the *HEC* cDNA clone. (B) Northern blot analysis of total RNA from 12 different sources: 1, CV1 monkey kidney cells; 2, human brain; 3, C4-I cervical carcinoma; 4, C4-II cervical carcinoma; 5, MS751 cervical carcinoma; 6, SiHa cervical carcinoma; 7, Caski cervical carcinoma; 8, Molt4 acute lymphocytic leukemia; 9, T47D breast carcinoma; 10, HT-3 cervical carcinoma; 11, SW620 colon carcinoma; 12, WERI-RB-27. The blot was probed with C15 and with Gβ-like cDNA, respectively. Gβ-like mRNA is expressed constitutively and therefore served as an internal control. The amounts of *HEC* mRNA relative to Gβ-like mRNA were determined by densitometry of the RNA blots. (C) *HEC* mRNA expression varies with progression of the cell cycle. CV1 monkey kidney cells were arrested at various phases of the cell cycle by serum deprivation or drug treatment. Lanes: 1, G_1 (density arrest, time zero); 2, late G_1 (8 h after release from density arrest); 3, G_1/S boundary (aphidicolin arrest); 4, S (4 h after release from aphidicolin arrest); 5, M (nocodazole arrest). E2F-1 mRNA expression, which peaks at G_1/S, and Gβ-like mRNA expression served as internal controls.

Cell fractionation. The procedures used to separate membrane, nuclear, and cytoplasmic fractions were adapted from those previously published (1). All three fractions were then assayed for Rb, a nuclear protein, and HEC by immunoprecipitation as described above. Aliquots of each fraction were also incubated with glutathione-agarose beads, separated by SDS-polyacrylamide gel electrophoresis and stained with Coomassie blue. The GST thus identified was used as a cytoplasmic marker.

Immunostaining. Cells grown on coverslips in tissue culture dishes were washed in phosphate-buffered saline (PBS) and fixed for 30 min in 4% formaldehyde in PBS with 0.5% Triton X-100. After being treated with 0.05% saponin in water for 30 min and extensively washed with PBS, the cells were blocked in PBS containing 10% normal goat serum. A 1-h incubation with suitable antibody diluted in 10% goat serum was followed by three washes and then by another 1-h incubation with fluorochrome-conjugated secondary antibody. Colocalization of HEC and centromere proteins (CENPs) was performed with a polyclonal mouse anti-HEC antibody mixed with human CREST autoimmune sera. The respective antigens were visualized with goat anti-human immunoglobulin G (IgG) or goat anti-rabbit IgG conjugated to Texas Red and goat anti-mouse IgG conjugated to fluorescein isothiocyanate. After being washed extensively in PBS with 0.5% Nonidet P-40, the cells were further stained with DAPI and mounted in Permafluor (Lipshaw-Immunonon, Inc., Pittsburgh, Pa.). Ektachrome P1600 film was used when the pictures were taken from a standard fluorescence microscope (Axiophot photomicroscope; Zeiss).

Microinjection with MAbs. The cells were injected, as described previously (18), with antibody solutions at 2 mg/ml in a microinjection buffer (20 mM phosphate buffer [pH 7.2], 0.1 mM EDTA, 10% glycerol), using Eppendorf's microinjection apparatus.

Nucleotide sequence accession number. The sequence reported herein has been deposited with GenBank under accession no. AF017790.

RESULTS

***HEC* mRNA is expressed abundantly in rapidly dividing cancer cells.** A 1.8-kb cDNA encoding C15 was originally isolated by a yeast two-hybrid screen for proteins that interact

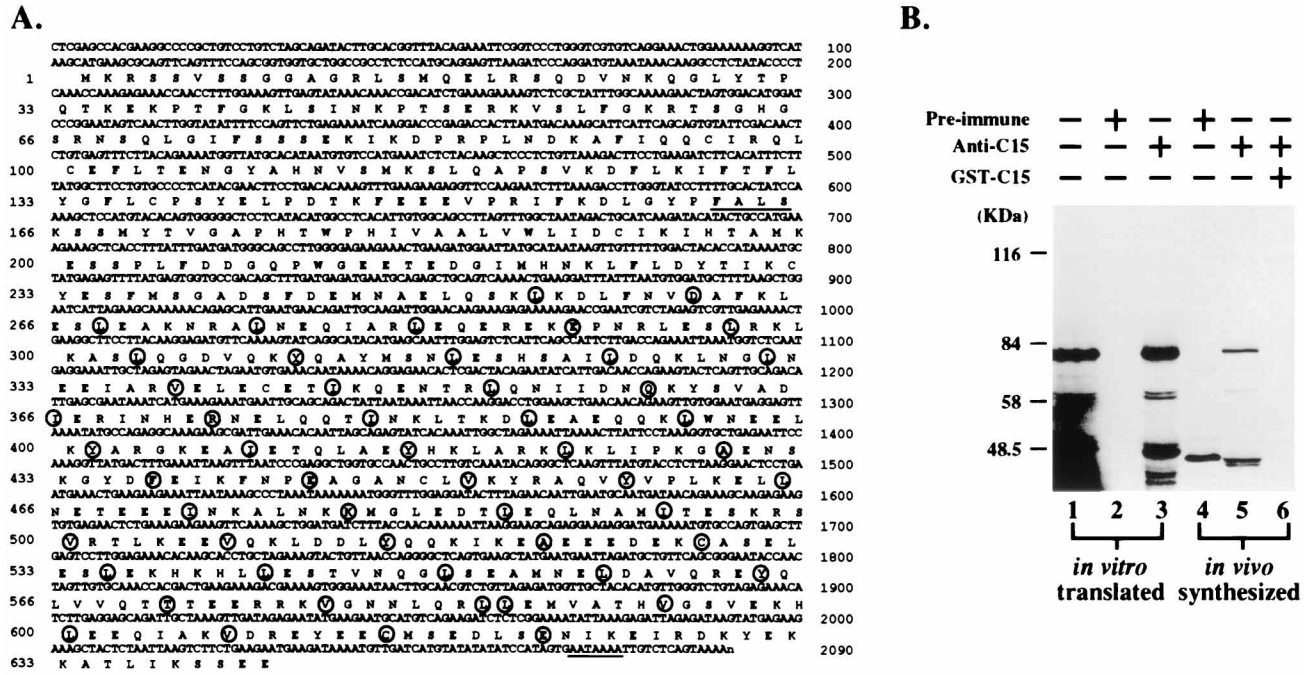

FIG. 2. Sequences of the HEC cDNA and its encoded protein. (A) Complete nucleotide sequence of the HEC cDNA. A potential NimA phosphorylation site (Ser 165) is underlined, and a long leucine heptad repeat sequence is marked with a series of circled residues. (B) A protein with an apparent molecular mass of 76 kDa was identified specifically by polyclonal anti-HEC serum. Mouse sera raised against a GST-C15 fusion protein were used to immunoprecipitate [^{35}S]methionine-labeled proteins, either from the in vitro-translated, full-length *HEC* cDNA (lanes 1 to 3) or from metabolically labeled T24 bladder carcinoma cells (lanes 4 to 6). In lanes 2 and 4, preimmune serum was used rather than anti-C15 antibodies. In lane 6, anti-C15 antibodies were preabsorbed with the GST-C15 antigen before immunoprecipitation.

with Rb (12). A single 2.3-kb mRNA species was found in all cells tested with the C15 fragment as a probe (Fig. 1A). Most of the tumor cell lines expressed C15 mRNA more abundantly than did normal tissues and untransformed cells (Fig. 1B). This expression pattern led to the name HEC (highly expressed in cancer). To test whether the expression in cells changed with progression of the cell cycle, RNA was prepared from synchronized CV1 monkey kidney cells at different time points after G_1 arrest. *HEC* mRNA expression varies with the cell cycle, increasing during S and M phases (Fig. 1C). This expression pattern is somewhat different from that of the transcription factor E2F-1, whose expression peaks at G_1/S and decreases in M (35). These results suggested that the protein encoded by *HEC* may play a role in cell proliferation.

***HEC* cDNA encodes a protein rich in leucine heptad repeats.** To obtain the full-length *HEC* cDNA, the original 1.8-kb C15 cDNA fragment was used as a probe to screen a human B-cell cDNA library. Several clones containing different fragments about 2 kb long were sequenced. The longest clone revealed an open reading frame encoding a 642-amino-acid protein with a predicted molecular mass of 72 kDa (Fig. 2A). This putative protein is acidic, with an isoelectric point of 5.5. A search of the updated GenBank database from the National Center for Biotechnology Information revealed no significant homology to any gene encoding a characterized protein. A striking feature of the sequence is its long series of typical leucine heptad repeats. These repeats span the region between amino acids 254 and 621, nearly two-thirds of the entire putative protein.

To identify the cellular protein encoded by *HEC*, polyclonal antibodies raised against a GST-C15 fusion protein were prepared. T24 bladder carcinoma cells were metabolically labeled with [^{35}S]methionine, and the cell lysates were processed for immunoprecipitation. Anti-HEC antibodies specifically immunoprecipitated a cellular protein that migrated in SDS-polyacrylamide gel electrophoresis with an apparent molecular mass of 76 kDa (Fig. 2B, lane 5). The protein was not detected by preimmune serum (lane 4). Furthermore, a GST-C15 fusion protein in the immunoprecipitation completely prevented precipitation of the cellular protein (lane 6). An unknown 46-kDa protein was coimmunoprecipitated. This could be a protein interacting with HEC (Fig. 2B, lane 5). When full-length *HEC* cDNA was used as template for in vitro transcription and translation, the synthesized protein was also immunoprecipitated by the same antibodies and migrated at the same position as the cellular protein (Fig. 2B, lane 3). These results show cellular HEC to be a 76-kDa protein and are consistent with the size predicted from the full-length *HEC* cDNA.

HEC protein is expressed in actively dividing cells but not in terminally differentiated cells. To evaluate the expression pattern of HEC, protein lysates prepared from different organs of an adult mouse were used for straight Western blot analysis (Fig. 3A). The HEC protein could be detected only in tissues with high mitotic indices, such as the testis, spleen, and thymus (Fig. 3A, upper panel). The internal control, a known nuclear matrix protein, p84 (13), was expressed in approximately equivalent amounts in all of these tissues (Fig. 3A, lower panel). The expression of HEC in tissues with high mitotic indices is consistent with the mRNA expression pattern and again suggested a potential role for HEC in proliferation in general or mitosis in particular. To investigate this notion further, the expression pattern of HEC was monitored during cell cycle progression. Cell lysates prepared from a synchronized population of T24 cells were analyzed by Western blotting with three different antibodies, MAb 11D7 (Rb) (35), anti-C15 (HEC), and anti-N5 (p84) (13). HEC protein was expressed in detectable amounts only in the late S to M phases (Fig. 3B).

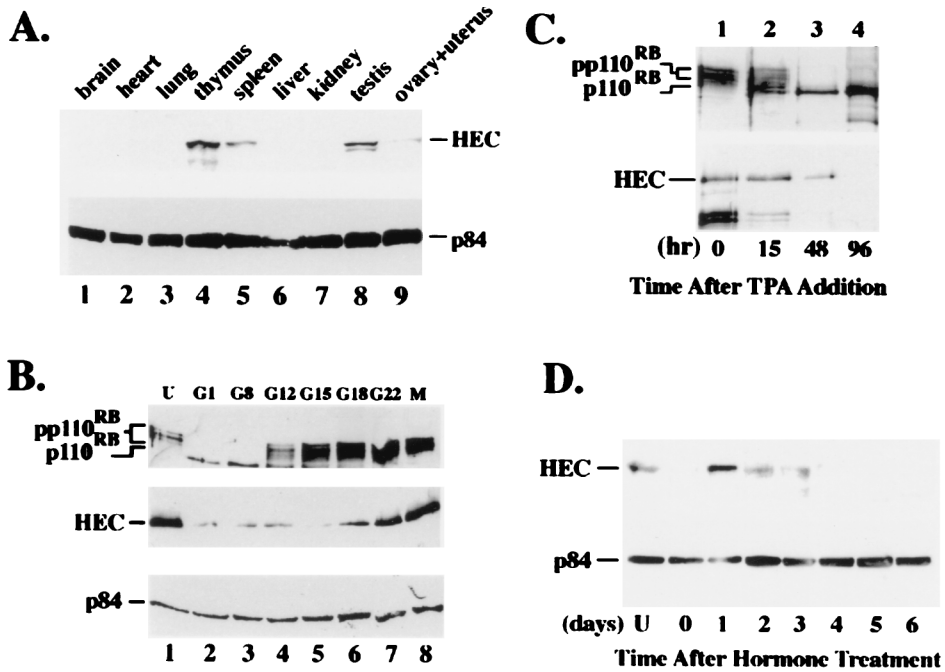

FIG. 3. HEC distribution in organs, rapidly dividing cells, and differentiating cells. (A) HEC protein expression in whole mouse organs. HEC immunoprecipitated from organ lysates was detected in thymus, spleen, testis, and ovary plus uterus. p84 served as a loading control. (B) HEC expression peaks in M phase. T24 cells were either unsynchronized (lane 1) or synchronized in G_1 and released for various periods (lanes 2 to 8; G8 = 8 h after release, etc.). Hypophosphorylated Rb ($p110^{RB}$) and various phosphorylated forms ($pp110^{RB}$) marked stages of the cell cycle: G_1 (lanes 2 to 5), G_1/S boundary (lane 6), S (lane 7), and M (lane 8). p84 again served as an internal control for protein loading. (C) U937 lymphoma cells in the exponential phase of proliferation were induced to differentiate by the addition of tetradecanoyl phorbol acetate. In rapidly dividing cells at time zero, Rb exists primarily in the hyperphosphorylated state ($pp110^{RB}$); after cell cycle arrest and terminal differentiation to monocytes/macrophages at 96 h, Rb is primarily hypophosphorylated ($p110^{RB}$). In contrast, HEC is present in proliferating cells but not in terminally differentiated cells. (D) Unsynchronized (U) NIH 3T3-L1 preadipocytes, identical cells synchronized at G_1/G_0 by density arrest (time zero) and cells induced to differentiate terminally to adipocytes by hormonal treatment (1 to 6 days after treatment) were analyzed in a manner similar to that used in panel C.

The Rb expression pattern in different cell cycle phases has been described previously (4) and served as a marker to confirm the phases of the cell cycle. p84 expression did not vary with progression of the cell cycle and served as an internal loading control (13). In rapidly dividing U937 large-cell lymphoma cells, HEC was expressed and detectable. When these cells were induced by phorbol ester to differentiate terminally into macrophages (6), however (Fig. 3C, lane 4), HEC expression became undetectable. Likewise, when murine 3T3/L1 cells were induced by appropriate hormones to differentiate into adipocytes (7) (Fig. 3D), HEC expression was easily detectable in dividing cells (Fig. 3D, lanes U and 1) but was undetectable in cells arrested at G_0/G_1 (lane 0) or in cells that had differentiated terminally (lanes 4 to 6). These results further strengthened the suggestion that HEC may function specifically in dividing cells.

HEC localizes in the nucleus and distributes to the centromere during mitosis. As the next step in exploring the potential function of HEC in dividing cells, we determined the subcellular location of HEC. Cells of the human bladder carcinoma cell line T24 were fractionated biochemically or fixed and immunostained with specific anti-HEC antibodies. In cells biochemically fractionated into nucleus, cytoplasm, and membrane components (1), HEC distributes mainly with the nuclear fraction (Fig. 4A). Rb, a nuclear protein, and GST, a cytoplasmic protein, served to control the fractionation procedure. The use of different immunostaining methods, including fixation with formaldehyde or methanol, showed that HEC also localized in the nucleus of the cell at G_1, in a speckled pattern (Fig. 4B, panel b). In S-phase cells, both perinuclear and nuclear staining were observed, probably due to the increase in HEC synthesis (Fig. 4B, panel d). In mitotic cells, a small portion of the protein localized as paired dots on chromosomes, while the majority was present in areas surrounding the chromosomes (Fig. 4B, panels f, h, j, and l). The majority of the HEC protein was probably degraded after mitosis (Fig. 4B, panels n and b). Staining of metaphase chromosome spreads revealed colocalization at the centromeres with CENPs, recognized by serum from a patient with autoimmune disease and CREST syndrome (30) (Fig. 4C). The use of preimmune serum resulted in the lack of any fluorescent signal, and the anti-HEC antibodies recognized only a single HEC protein by straight Western blotting analysis (see below), indicating that the immunostaining pattern specifically reflects the HEC protein. These results show HEC to be a nuclear, centromere-associated protein and again suggest a role for HEC in M phase.

Cells microinjected with anti-HEC antibodies divide aberrantly to form fragmented nuclei. To test directly whether HEC is important functionally for M phase, a specific MAb recognizing HEC was prepared and microinjected into cultured cells to inactivate endogenous HEC. Mouse MAb 9G3 was generated by the same GST-C15 fusion protein immunogen used to make the polyclonal antiserum. This MAb was specific for HEC in immunoprecipitation and in straight immunoblotting (Fig. 5A); it recognized the same 76-kDa protein as the polyclonal anti-HEC serum.

For the microinjection studies, T24 human bladder carcinoma cells were synchronized in S phase and microinjected with MAb 9G3. At 26 h later, at a time when all the cells should

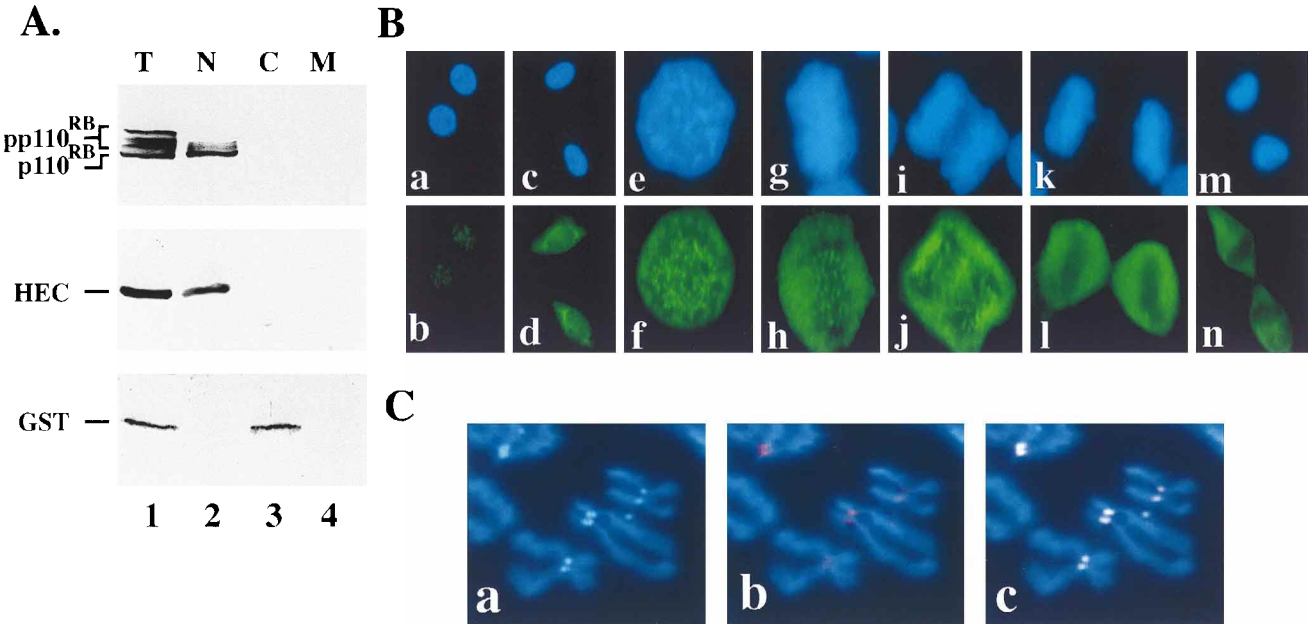

FIG. 4. Subcellular localization of HEC. (A) Biochemical fractionation of T24 cells (T) into nuclear (N), cytoplasmic (C), and membrane (M) components. Each fraction was immunoprecipitated by either anti-C15 (HEC) antibodies or 11D7 anti-Rb MAb. Rb detected from the same cells served as a marker for nuclear protein. The same subcellular fractions were also incubated with glutathione-agarose beads to identify GST, which served as a marker for cytoplasmic proteins. (B) Panels a, c, e, g, i, k, and m show DAPI fluorescence; panels b, d, f, h, j, l, and n show anti-HEC staining. Immunocytochemical localization during different phases of the cell cycle is shown. Panels: a and b, T24 cells fixed in late G_1 phase show scanty staining in nuclei (magnification, ×344); c and d, cells in S phase stained in perinuclear and nuclear locations; e to j, cells in metaphase (higher magnification, ×860) show strong staining surrounding the chromosomes as well as paired dots on the chromosomes; k and l, a cell in telophase shows strong staining surrounding the chromosomes; m and n, cells after cytokinesis showing weaker staining surrounding the chromosomes. (C) Metaphase chromosomes were first stained with DAPI. The same microscopic field was then analyzed after indirect immunofluorescent-antibody staining. Panels: a, anti-C15 polyclonal serum (1:1,000 dilution) and FITC-tagged anti-mouse IgG secondary antibodies localized HEC to centromeres; b, human polyclonal autoimmune (CREST) antiserum, which recognizes centromere proteins, and Texas Red-tagged secondary antibodies also labeled centromeres; c, digital overlay of anti-C15 and CREST antiserum images.

have completed mitosis, the majority of cells injected with MAb 9G3 contained multiple, fragmented nuclei. Uninjected cells and those injected with the control antibody (total murine IgG) divided into two normal daughter cells (Fig. 5B). Many cells injected with anti-HEC antibodies were missing and presumed dead 26 h after injection. The results of three separate experiments were consistent (Table 1).

M-phase progression in cells injected with anti-HEC MAbs was observed closely to determine more precisely the events responsible for the appearance of abnormal nuclei and apparent cell death. Chromosomes in anti-HEC-injected cells condensed but failed to coalesce or segregate properly (Fig. 5C). No distinct metaphase plates were observed, and spindles were disorganized in relation to their centromeres (Fig. 5C, panels g to l). In many cells, multiple spindle poles were observed (panels g and h). Superimposition of images of the same cells stained with DAPI (to identify chromosomes) and with an antibody recognizing tubulin (to identify the spindle apparatus) showed that many spindles failed to assume the proper orthogonal orientation to their chromatids (panels k and l). Cells injected with anti-HEC antibodies were able to undergo cytokinesis, but chromosomes separated haphazardly into grossly abnormal daughter cells which were ultimately nonviable. Similar results were obtained by injecting the anti-HEC antibody into cells synchronized in the G_1 phase (data not shown).

DISCUSSION

Several lines of evidence indicate that HEC may be an important protein for M-phase progression. First, HEC is expressed most abundantly in mitotic cells but not in those that have terminally differentiated. Second, a portion of HEC redistributes to the centromeres of dividing cells. Third, inactivation of HEC by microinjection with specific antibodies severely disturbs chromosome distribution. These results suggest that HEC may be involved in chromosome segregation during M phase progression.

Abnormalities observed during metaphase and anaphase can result from primary problems earlier in the cell cycle. Microinjection of polyclonal CREST serum, which recognizes several different centromeric proteins, for example, is known to disrupt kinetochore assembly and to block progression through mitosis (3, 36). The timing of the antiserum injection in such experiments was crucial. If injected into the cytoplasm or nucleus during S or G_2 phases, anti-centromere antibodies caused abnormalities in mitosis very similar to those described here after injection of specific anti-HEC antibodies. In contrast, if injected into nuclei after alignment of metaphase chromatids had been completed, anti-centromere antibodies had little effect on the subsequent progression of mitosis (3).

In the present study, anti-HEC antibodies were microinjected into cells during S phase, and nuclear morphology was determined 26 h later, when all the cells should have completed mitosis. We cannot exclude prolongation of M phase in cells injected with MAb 9G3, but cells fixed after the completion of abnormal mitosis nonetheless underwent karyokinesis and cytokinesis. In normal cells, "wait anaphase" checkpoints sense tension and kinetochore attachments to microtubules (reviewed in reference 32). These checkpoints normally delay or prevent completion of mitosis in cells with inaccurate or incomplete division of chromosomes to daughter cells (32). In

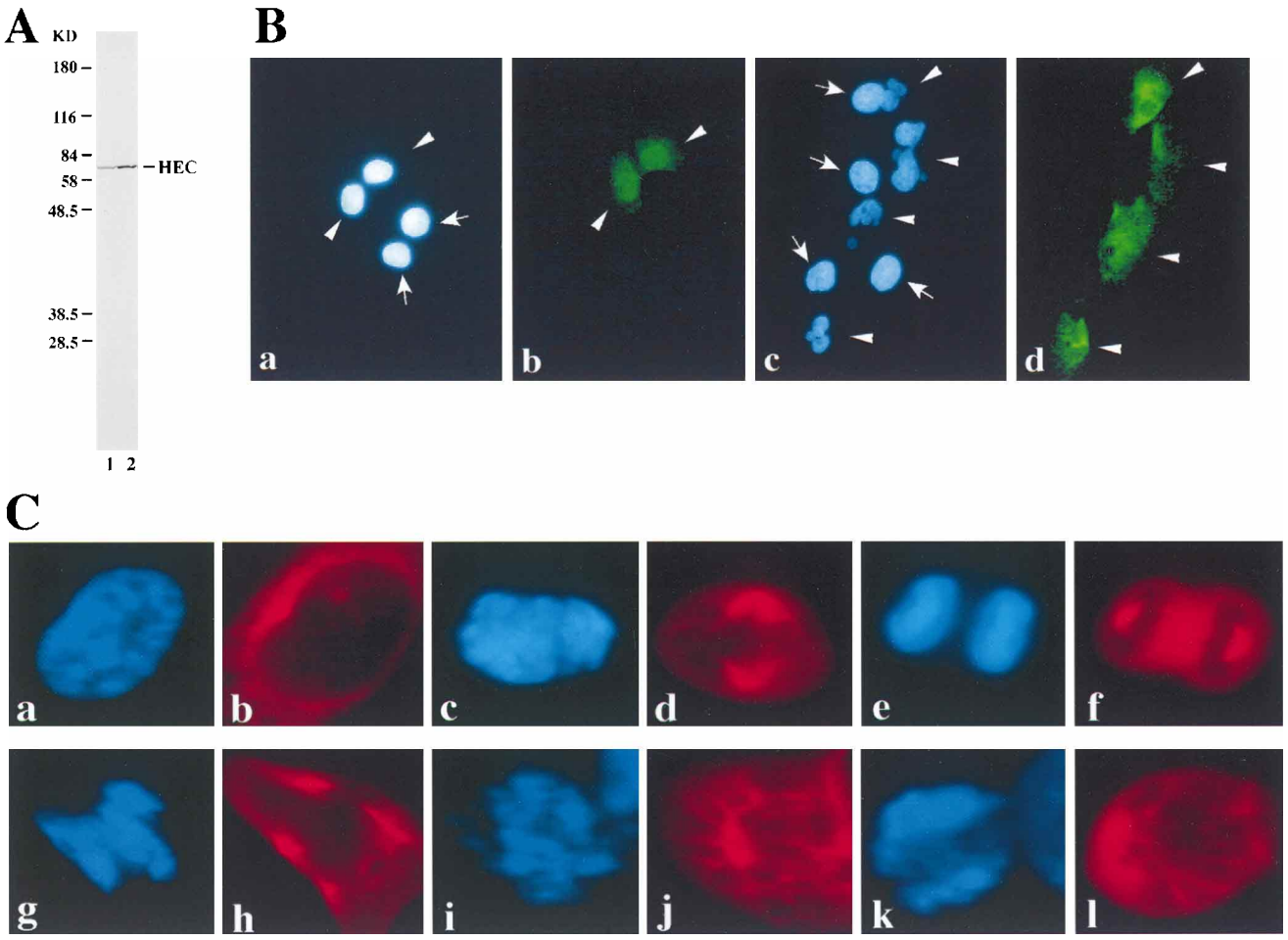

FIG. 5. Microinjection of anti-HEC results in aberrant mitosis. (A) Characterization of mouse MAb 9G3. The antibody was generated against the same antigen used to make polyclonal anti-C15 and used for straight immunoblotting of protein lysates from 5×10^5 CV1 (lane 1) or T24 (lane 2) cells. (B) T24 cells were released from density arrest and allowed to proceed through the cell cycle. At 24 h after release, the majority of cells were in S phase, at which time they were microinjected with either nonspecific mouse IgG (panels a and b) or MAb 9G3 (panels c and d). At 26 h later, after they should have passed through mitosis, the cells were fixed and analyzed by indirect immunofluorescent-antibody staining. Panels: a and c, DAPI fluorescence; b and d, staining with anti-mouse IgG antibodies. The arrowheads in each panel identify the daughters of cells that were successfully microinjected. The daughter cells marked by arrows in panels a and c were not microinjected. (C) Cells at different phases of mitosis. Panels a to f show normal mitosis in uninjected cells or cells microinjected with control mouse IgG; panels g to l show mitotic phases of cells injected with anti-HEC MAb 9G3. Blue fluorescence is from DAPI, which binds to DNA specifically; red fluorescence is from rabbit anti-tubulin primary antibody and Texas Red-conjugated anti-rabbit IgG secondary antibody to indicate the spindle behavior. Panels: a and b, prophase; c and d, metaphase; e and f, early telophase; g and h, abnormal spindle formation with at least four discrete spindle poles; i and j, disordered chromatid alignment and absence of a distinct metaphase plate; k and l, abnormal chromatid segregation: the chromatids in panel k align along a nearly horizontal axis, but the corresponding spindles in panel l pull in a direction 90° different.

anti-HEC-injected cells, such checkpoints appear to be partially or completely bypassed. This finding indicates that HEC may play roles other than those directly related to spindle attachment at the centromere. Abnormal conditions in the spindle apparatus, whose morphology probably dictates the location of the cleavage furrow during cytokinesis (3), might explain the bypass of normal checkpoints.

Proteins with properties similar to those of HEC have been characterized. The nuclear protein that associates with the mitotic apparatus (NuMA), for example, is also required for the proper completion of mitosis (9). When NuMA is inactivated, either by strategic mutation or by microinjection of anti-NuMA antibodies prior to mitosis, abnormalities in chromosome alignment and segregation result in the formation of daughter cells with micronuclei very similar to those reported here after HEC inactivation (9, 14, 28). Furthermore, several features of the abnormal mitotic phenotype observed after inactivation of HEC—particularly the multiple spindle poles and disordered metaphase chromosome alignment—can also be seen in mammalian cells treated with drugs, such as taxol and vinca alkaloids, that directly disrupt microtubule structure (26, 27). These drugs, however, all arrest cells in M phase, as does the injection of neutralizing antibodies to all known CENPs. In contrast, HEC inactivation does not arrest cells in mitosis but allows them to proceed aberrantly. This observation implies that there is a problem with checkpoint control in cells in which HEC has been inactivated.

The mechanism by which HEC functions prior to and during mitosis has yet be fully determined. The location of a subset of HEC at the centromere/kinetochore indicates that the protein may be involved in spindle attachment to chromosomes during prophase and indirectly in subsequent chromosome movement. The lack of a signature tubulin-binding domain in the HEC molecule, however, argues against direct microtubule attachment. Results from our further study indicate that many of the HEC-associated proteins isolated by a yeast two-hybrid

TABLE 1. Summary of results from microinjection of T24 cells with anti-HEC MAb 9G3

Expt no.	Injected antibody	No. of cells:			
		Divided cells		Undivided cells	Total
		Abnormal	Normal		
1	Mouse IgG	0	122	22	144
	MAb 9G3	108	0	27	135
2	Mouse IgG	0	76	16	92
	MAb 9G3	58	0	16	74
3	Mouse IgG	0	171	28	199
	MAb 9G3	92	0	13	105
Total	Mouse IgG	0	369	66	435
	MAb 9G3	258	0	56	314

screen are subunits of the proteasome (8a). The dynamics of the spindle apparatus are modulated, at least in part, by the same components of the proteasome and ubiquitin-dependent protein degradation pathway with which HEC seems to interact (24, 25, 29, 41). The interaction between HEC and proteasome provides a potential clue to how HEC influences chromosome congression, separation, or segregation.

A link between Rb and M-phase progression? In preliminary experiments, we have used an in vitro binding assay to determine a specific region near the N terminus of HEC that binds to Rb in its T-antigen-binding domain (data not shown). Similarly, HEC and Rb can be coimmunoprecipitated reciprocally only in M phase. These findings suggest that the interaction between HEC and Rb is indeed specific. However, the biological significance of such an interaction is unknown. Cells without Rb can successfully proceed through the cell cycle, and therefore an interaction between HEC and Rb is not absolutely required for M-phase progression. If there is a consequence of such an interaction, it is probably subtle, e.g., in checking the accuracy and timing of chromosome segregation. Interestingly, three other important proteins involved in M-phase progression, phosphatase 1α, H-nuc(cdc27), and mitosin, are associated with hypophosphorylated Rb (5, 12, 47). Accumulating evidence, including the data presented here, has led us to hypothesize a potential role for Rb in influencing the fidelity of chromosome segregation during mitosis (33, 47). The biological consequence of the interaction of Rb with HEC can now be explored to shed light on the possible role of Rb protein in mitotic processes.

ACKNOWLEDGMENTS

We thank B. Brinkley for the CREST antiserum, D. Jones for assistance in the production of antibodies, and several colleagues in our laboratory for helpful comments.

This work was supported by grants from the National Institutes of Health (EY05758 and CA58318) and the Council for Tobacco Research.

REFERENCES

1. **Abrams, H. D., R. Rohrscheider, and N. Eisenman.** 1982. Nuclear location of the putative transforming protein of avian myelocytomatosis virus. Cell **29:** 427–439.
2. **Bai, C., M. Sen, K. Hofmann, L. Ma, M. Goebl, J. W. Harper, and S. J. Elledge.** 1996. *SKP1* connects cell cycle regulators to the ubiquitin proteolysis machinery through a novel motif, the F-box. Cell **86:**263–274.
3. **Bernat, R. L., G. G. Borisy, N. F. Rothfield, and W. C. Earnshaw.** 1990. Injection of anticentromere antibodies in interphase disrupts events required for chromosome movement at mitosis. J. Cell. Biol. **111:**1519–1533.
4. **Chen, P.-L., P. Scully, J.-Y. Shew, J. Y. J. Wang, and W.-H. Lee.** 1989. Phosphorylation of the retinoblastoma gene product is modulated during the cell cycle and cellular differentiation. Cell **58:**1193–1198.
5. **Chen, P.-L., Y.-C. Ueng, T. Durfee, K.-C. Chen, T. Yang-Feng, and W.-H. Lee.** 1995. Identification of a human homologue of yeast nuc2 which interacts with the retinoblastoma protein in a specific manner. Cell Growth Differ. **6:**199–210.
6. **Chen, P.-L., D. J. Riley, S. Chen-Kiang, and W.-H. Lee.** 1996. Retinoblastoma protein directly interacts with and activates the transcription factor NF-IL6. Proc. Natl. Acad. Sci. USA **93:**465–469.
7. **Chen, P.-L., D. J. Riley, Y. Chen, and W.-H. Lee.** 1996. Retinoblastoma protein positively regulates terminal adipocyte differentiation through direct interaction with C/EBPs. Genes Dev. **10:**2794–2804.
8. **Chen, Y., A. A. Farmer, C.-F. Chen, D. C. Jones, P.-L. Chen, and W.-H. Lee.** 1996. BRCA1 is a 220-kDa nuclear phosphoprotein that is phosphorylated in a cell cycle-dependent manner. Cancer Res. **56:**3168–3172.

8a. **Chen, Y., Z. D. Sharp, and W.-H. Lee.** HEC binds to the seventh regulatory subunit of 265 proteasome and modulates the degradation of mitotic cyclins. J. Biol. Chem., in press.

9. **Compton, D. A., and D. W. Cleveland.** 1993. NuMA is required for the proper completion in mitosis. J. Cell Biol. **120:**947–957.
10. **Deshaies, R. J.** 1995. The self-destructive personality of a cell cycle in transition. Curr. Opin. Cell Biol. **7:**781–789.
11. **Doonan, H. J., and N. R. Morris.** 1989. The bimG gene of Aspergillus nidulans, which is required for completion of anaphase, encodes a homolog of mammalian phosphoprotein phosphatase 1. Cell **57:**987–996.
12. **Durfee, T., K. Becherer, P.-L. Chen, S.-H. Yeh, Y. Yang, W.-H. Lee, and S. J. Elledge.** 1993. The retinoblastoma protein associates with the protein phosphatase type 1 catalytic subunit. Genes Dev. **7:**555–569.
13. **Durfee, T., M. A. Mancini, D. Jones, S. J. Elledge, and W.-H. Lee.** 1994. The amino terminal region of the retinoblastoma gene product binds a novel nuclear matrix protein that localizes to RNA processing centers. J. Cell Biol. **127:**609–622.
14. **Gaglio, T., A. Seredi, and D. A. Compton.** 1995. NuMA is required for the organization of microtubules into aster-like mitotic arrays. J. Cell Biol. **131:** 693–708.
15. **Ghislain, M., A. Udvardy, and C. Mann.** 1993. S. cerevisiae 26S protease mutants arrest cell division in G2/metaphase. Nature **366:**358–361.
16. **Glotzer, M., A. W. Murray, and M. W. Kirschner.** 1991. Cyclin is degraded by the ubiquitin pathway. Nature **349:**132–138.
17. **Goebl, M., and M. Yanagida.** 1991. The TPR snap helix: a novel protein repeat motif from mitosis to transcription. Trends Biochem. Sci. **16:**173–177.
18. **Goodrich, D. W., N. P. Wang, Y.-W. Qian, E. Y.-H. P. Lee, and W.-H. Lee.** 1991. The retinoblastoma gene product regulates progression through G1 phase of the cell cycle. Cell **67:**293–302.
19. **Harlow, E., and D. Lane.** 1988. Antibodies: a laboratory manual, p. 139–243. Cold Spring Harbor Laboratory Press, Cold Spring Harbor, N.Y.
20. **Harper, J. W., and S. J. Elledge.** 1995. Cdk inhibitors in development and cancer. Curr. Opin. Genet. Dev. **6:**56–64.
21. **Hartwell, L.** 1992. Defects in a cell cycle checkpoint may be responsible for the genomic instability of cancer cells. Cell **71:**543–546.
22. **He, D., C. Zeng, and B. R. Brinkley.** 1995. Nuclear matrix proteins as structural and functional components of the mitotic apparatus. Int. Rev. Cytol. **162B:**1–74.
23. **Hirano, T., Y. Niraoka, and M. Yanagida.** 1988. A temperature-sensitive mutation of Schizosaccharomyces pombe gene nuc2+ that encodes a nuclear scaffold-like protein blocks spindle elongation in mitotic anaphase. J. Cell Biol. **106:**1171–1183.
24. **Holloway, S. L., M. Glotzer, R. W. King, and A. W. Murray.** 1993. Anaphase is initiated by proteolysis rather than by the inactivation of maturation-promoting factor. Cell **73:**1393–1402.
25. **Irniger, S., S. Piatti, C. Michaelis, and K. Nasmyth.** 1995. Genes involved in sister chromatid separation are needed for B-type cyclin proteolysis in budding yeast. Cell **81:**269–277.
26. **Jordan, M. A., R. J. Toso, D. Thrower, and L. Wilson.** 1993. Mechanism of mitotic block and inhibition of cell proliferation by taxol at low concentrations. Proc. Natl. Acad. Sci. USA **90:**9552–9556.
27. **Jordan, M. A., D. Thrower, and L. Wilson.** 1992. Effects of vinblastine, podophyllotoxin and nocodazole on mitosis spindles. Implications for the role of microtubule dynamics in mitosis. J. Cell Sci. **102:**401–416.
28. **Kallajoki, M., J. Harborth, K. Weber, and M. Osborn.** 1993. Microinjection of a monoclonal antibody against SPN antigen, now identified by peptide sequences as the NuMA protein, induces micronuclei in PtK2 cells. J. Cell Sci. **104:**139–150.
29. **King, R. W., J. M. Peters, S. Tugenreich, M. Rolfe, P. Heiter, and M. W. Kirschner.** 1995. A 20S complex containing CDC27 and CDC16 catalyzes the mitosis-specific conjugation of ubiquitin to cyclin B. Cell **81:**279–288.
30. **Moroi, Y., C. Peebles, M. J. Fritzler, J. Steigerwald, and E. M. Tam.** 1980. Autoantibody to centromere (kinetochore) in scleroderma sera. Proc. Natl. Acad. Sci. USA **77:**1627–1631.
31. **Osmani, S. A., R. T. Pu, and N. R. Morris.** 1988. Mitotic induction and maintenance by overexpression of a G2-specific gene that encodes a poten-

tial protein kinase. Cell **53:**237–244.
32. **Pluta, A. F., A. M. Mackay, A. M. Ainsztein, I. G. Goldberg, and W. C. Earnshaw.** 1995. The centromere: hub of chromosomal activities. Science **270:**1591–1594.
33. **Riley, D. J., E. Y.-H. P. Lee, and W.-H. Lee.** 1994. The retinoblastoma protein: more than a tumor suppressor. Annu. Rev. Cell. Biol. **10:**1–29.
34. **Samejima, I., and M. Yanagida.** 1994. Bypassing anaphase by fission yeast cut9 mutation: requirement of cut9+ to initiate anaphase. J. Cell Biol. **127:**1655–1670.
35. **Shan, B., X. Zhu, P.-L. Chen, T. Durfee, Y. Yan, D. Sharp, and W.-H. Lee.** 1992. Molecular cloning of cellular genes encoding retinoblastoma-associated proteins: identification of a gene with properties of the transcription factor E2F. Mol. Cell. Biol. **12:**5620–5631.
36. **Simerly, C., R. Balczon, B. R. Brinkley, and G. Schatten.** 1990. Microinjected centromere/kinetochore antibodies interfere with chromosome movement in meiosis and mitotic mouse oocytes. J. Cell Biol. **111:**1491–1504.
37. **Solomon, E., J. Borrow, and A. D. Goddard.** 1991. Chromosome aberrations and cancer. Science **254:**1153–1160.
38. **Strunnikov, A. V., U. L. Larionov, and D. Koshland.** 1993. SMC1: an essential yeast gene encoding a putative head-rod-tail protein is required for nuclear division and defines a new ubiquitous protein family. J. Cell Biol. **123:**1635–1648.
39. **Strunnikov, A. V., E. Hogan, and D. Koshland.** 1995. SMC2, a Saccharomyces cerevisiae gene essential for chromosome segregation and condensation, defines a subgroup within the SMC family. Genes Dev. **9:**587–590.
40. **Swaffield, J. C., J. F. Bromberg, and S. A. Johnston.** 1992. Alterations in a yeast protein resembling HIV Tat-binding protein relieve requirement for an acidic activation domain in GAL4. Nature **357:**698–670.
41. **Tugenreich, S., J. Tomkiel, W. Earnshaw, and P. Heiter.** 1995. CDC27Hs colocalizes with CDC16Hs to the centrosome and mitotic spindle and is essential for the metaphase to anaphase transition. Cell **81:**261–268.
42. **Walczak, C. Z., and T. J. Mitchison.** 1996. Kinesin-related proteins at mitotic spindle poles: function and regulation. Cell **85:**943–946.
43. **Wang, Y., and D. J. Burke.** 1995. Checkpoint genes required to delay cell division in response to nocodazole respond to impaired kinetochore function in the yeast *Saccharomyces cerevisiae.* Mol. Cell. Biol. **15:**6838–6844.
44. **Weisenberg, R. C., and A. C. Rosenfeld.** 1975. In vitro polymerization of microtubules into asters and spindles in homogenates of surf clam eggs. J. Cell Biol. **64:**146–158.
45. **Wells, W. A. E., and A. W. Murray.** 1996. Aberrantly segregating centromeres activate the spindle assembly checkpoint in budding yeast. J. Cell Biol. **133:**75–84.
46. **Yanagida, M.** 1995. Frontier questions about sister chromatid separation in anaphase. Bioessays **17:**519–526.
47. **Zhu, X., M. A. Mancini, K. H. Chang, C.-Y. Liu, C.-F. Chen, T. L. Yang-Feng, and W.-H. Lee.** 1995. Characterization of a novel 350-kilodalton nuclear phosphoprotein that is specifically involved in mitotic phase progression. Mol. Cell. Biol. **15:**5017–5029.